

**BUCKLING ANALYSIS OF CSCS AND CSSS RECTANGULAR PLATES BY SPLIT-DEFLECTION METHOD**

<sup>1</sup> Momoh Habib <sup>2</sup>J.O. Onyeka, and <sup>3</sup>H.E. Opara

<sup>1, 2 & 3</sup>, Civil Engineering Department, Imo State University, Owerri, Nigeria

**Abstract**—This paper presents buckling analysis of cscs and csss rectangular plates by split-deflection method. The assumption was that the deflection,  $w$  is split into  $w_x w_y$ ; where the deflection was taken as the product of these two components in  $x$  and  $y$  directions. The study formulated the total potential energy function from principles of theory of elasticity. By direct variation, the energy function was minimized and equations for critical buckling loads were obtained. Two examples, one with edges 1 and 3 clamped, edges 2 and 4 simply supported and the other with edges 2, 3 and 4 simply supported and edge 1 clamped were used to test this method. The use of polynomial functions for both  $x$  and  $y$  components of deflection was adopted. Critical buckling loads (in non-dimensional forms) of the two examples for aspect ratios ranging from 1.0 to 2.0 (at increment of 0.1) were determined and compared with the values from previous study (Ibearugbulem et al., 2014). From the comparison, it was observed that the maximum percentage difference of 0.196 was recorded. The small values of percentage difference from this study show that this present method is sufficient and reliable for classical plate theory (CPT) buckling analysis of rectangular plates.

**Index Terms**—Critical buckling load, split-deflection, work-error, energy function, polynomial function.

**INTRODUCTION**

Classical plate theory (CPT) buckling analysis has dominated energy methods such as Raleigh, Ritz, Galerkin, minimum potential energy, etc (Ugural, 1999, Ventsel and Krauthammer, 2001 and Ibearugbulem et al., 2014). Most of these energy methods are characterized by single deflection (un-separated) function. For instance, let us look at the energy function of work error method (Ibearugbulem et al., 2014):

$$U = \frac{1}{2} \int_0^a \int_0^b \left( \frac{D^4 w^4}{2^4} + 2 \frac{D^4 w^2}{2^2 2^2} + \frac{D^4 w^2}{2^2 2^4} \right) dx dy - \frac{1}{2} \int_0^a \int_0^b q^2 dx dy$$

Most academic works on CPT analysis of rectangular plates as seen from the literature rely on this single orthogonal function (Hutchinson, 1992, Jianqiao, 1994, Ugural, 1999, Ventsel and Krauthammer, 2001, Wang et al., 2002, Taylor and Govindjee, 2004, Szilard, 2004, Jiu et al., 2007, Erdem et al., 2007, Ezeh et al., 2013, Ibearugbulem, 2014). Evidently, it can be affirmed that all energy functions currently in use in CPT buckling analysis are based on this single orthogonal deflection function. This means that none of the existing energy functions for buckling analysis in CPT has used a deflection function that is classically separated into two independent and distinct functions ( $w = w_x * w_y$ ) where  $w_x$  and  $w_y$  are both polynomial functions or  $w_x$  may be polynomial while  $w_y$  may be trigonometry. The rationale for this adaptation is to help the analyst who might have difficulty in obtaining single orthogonal function for a plate of a particular boundary condition. In this case, the analyst who may have easy access to deflection equations for beams of any boundary condition can find this proposed method very handy.

**ASSUMPTIONS**

**1. Basic-** The hypothesis here is that the general deflection,  $w$  is split into  $w_x$  and  $w_y$ . That is, the split-deflection function is given as:

$$w = w_x + w_y \dots \dots \dots \tag{1}$$

where the  $w_x$  and  $w_y$  components of the deflection are defined as:

$$w_x = \sqrt{a} \cdot w_1 \dots \dots \dots \tag{2}$$

$$w_y = \sqrt{a} \cdot w_2 \dots \dots \dots \tag{3}$$

$$w = \sqrt{a} \cdot w_1 \cdot \sqrt{a} \cdot w_2$$

Applying split-deflection and substituting equations (2) and (3) into equation (1) gives:

$$w = a w_1 w_2 \dots \dots \dots \tag{4}$$

**2. In-Plane Displacements-** From the hypothesis that vertical shear strains are zero for classical plates and making use of split-deflection approach, we obtain:

$$u = -a \frac{\partial^2 w}{\partial x^2} = -a \frac{\partial^2 (a w_1 w_2)}{\partial x^2} \dots \dots \dots \tag{5}$$

$$v = -a \frac{\partial^2 w}{\partial y^2} = -a \frac{\partial^2 (a w_1 w_2)}{\partial y^2} \dots \dots \dots \tag{6}$$

**3. Strain Deflection Relationship-** Upon differentiating equations (5 and (6), the three in-plane strains of CPT are obtained:

$$\epsilon_x = \frac{\partial u}{\partial x} = -a \frac{\partial^3 (a w_1 w_2)}{\partial x^3} \dots \dots \dots \tag{7}$$

$$\epsilon_y = \frac{\partial v}{\partial y} = -a \frac{\partial^3 (a w_1 w_2)}{\partial y^3} \dots \dots \dots \tag{8}$$

$$\epsilon_{xy} = \frac{\partial u}{\partial y} + \frac{\partial v}{\partial x} = -2a \frac{\partial^3 (a w_1 w_2)}{\partial x \partial y^2} \dots \dots \dots \tag{9}$$

**4. Stress-Strain Relationship-**The CPT constitutive equations for plane stress plates are:

$$\epsilon_x = \frac{1}{1 - \nu^2} [\sigma_x + \nu \sigma_y] \dots\dots 10$$

$$\epsilon_y = \frac{1}{1 - \nu^2} [\nu \sigma_x + \sigma_y] \dots\dots 11$$

$$\gamma_{xy} = \frac{2(1 - \nu)}{2(1 - \nu^2)} \tau_{xy} \dots\dots 12$$

**DERIVATION OF CRITICAL BUCKLING LOAD EQUATION USING SPLIT**

**DEFLECTION METHOD**

**1. Stress-Deflection Relationship-** When equations (7), (8) and (9) are substituted into equations (10), (11) and (12) as appropriate, the split-deflection stress-deflection equations are obtained as:

$$\sigma_x = \frac{-\nu \tau_{xy}}{1 - \nu^2} \left[ \frac{\tau_{xy}^2}{\tau_{xy}^2} \epsilon_x + \frac{\tau_{xy}^2}{\tau_{xy}^2} \epsilon_y \right] \dots\dots 13$$

$$\sigma_y = \frac{-\nu \tau_{xy}}{1 - \nu^2} \left[ \frac{\tau_{xy}^2}{\tau_{xy}^2} \epsilon_x + \frac{\tau_{xy}^2}{\tau_{xy}^2} \epsilon_y \right] \dots\dots 14$$

$$\tau_{xy} = \frac{-\nu \tau_{xy} (1 - \nu) \tau_{xy} \tau_{xy}}{(1 - \nu^2) \tau_{xy} \tau_{xy}} \dots\dots 15$$

**2. Total Potential Energy-** Strain energy is commonly defined as:

$$U = \frac{1}{2} \int_{-a/2}^{a/2} \int_{-b/2}^{b/2} \left[ \int_{-c/2}^{c/2} [\sigma_x \epsilon_x + \sigma_y \epsilon_y + \tau_{xy} \gamma_{xy}] dz \right] dx dy \dots\dots 16$$

For buckling analysis, the external work in x direction is given as:

$$W = \frac{\tau_{xy}}{2} \int_{-a/2}^{a/2} \int_{-b/2}^{b/2} \frac{\tau_{xy}^2}{\tau_{xy}^2} dx dy$$

That is,

$$= \frac{1}{2} \int_0^L \left[ \frac{EI}{2} \left( \frac{d^2 w}{dx^2} \right)^2 + \dots \right] dx \tag{17}$$

When equations (4) to (6) are substituted into equation (7) we obtain strain energy – deflection equation form as:

$$= \frac{1}{2} \left[ \int_0^L \frac{EI}{2} \left( \frac{d^2 w}{dx^2} \right)^2 dx + \frac{2EI}{2} \left[ \int_0^L \frac{d^2 w}{dx^2} \frac{dw}{dx} dx + \int_0^L \frac{d^2 w}{dx^2} w dx \right] + \frac{1}{2} \left[ \int_0^L w^2 dx + \int_0^L \frac{d^4 w}{dx^4} w dx \right] \dots \right] \tag{18}$$

Adding equations (17) and (18) give the total potential energy function as:

$$= \frac{1}{2} \left[ \int_0^L \frac{EI}{2} \left( \frac{d^2 w}{dx^2} \right)^2 dx + \frac{2EI}{2} \left[ \int_0^L \frac{d^2 w}{dx^2} \frac{dw}{dx} dx + \int_0^L \frac{d^2 w}{dx^2} w dx \right] + \frac{1}{2} \left[ \int_0^L w^2 dx + \int_0^L \frac{d^4 w}{dx^4} w dx \right] + \frac{1}{2} \int_0^L \frac{d^2 w}{dx^2} w dx \dots \right] \tag{19}$$

When equations (2) and (3) are substituted into equation (19) we obtain:

$$= \frac{EI}{2} \left[ \int_0^L \frac{d^4 w_1}{dx^4} w_1 dx + \int_0^L \frac{d^4 w_2}{dx^4} w_2 dx \right] + \frac{2EI}{2} \left[ \int_0^L \frac{d^2 w_1}{dx^2} w_1 dx + \int_0^L \frac{d^2 w_2}{dx^2} w_2 dx \right] + \frac{1}{2} \left[ \int_0^L w_1^2 dx + \int_0^L \frac{d^4 w_2}{dx^4} w_2 dx \right] + \frac{1}{2} \int_0^L \frac{d^2 w}{dx^2} w dx \dots \tag{20}$$

Using non-dimensional form of axes R and Q, equation (20) shall be written as:

$$= \dots \tag{21}$$

$$= \dots \tag{22}$$

$$\frac{\delta U}{\delta A} = \dots\dots\dots$$

Here a, b and P are the plate lengths in x and y axes and long span- short span aspect ratio respectively.

When equations (21), (22) and (23) are substituted into equation (20) we obtain:

$$\begin{aligned} &= \frac{P^2 a^2 b^2}{2P^4} \left[ \int_0^1 \frac{P^4 a_1^2}{P^4} a_1^2 \int_0^1 P^2 a_2^2 \right] \\ &\quad + 2 \frac{P^2 a^2 b^2}{2P^4 P^2} \left[ \int_0^1 \frac{P^2 a_1^2}{P^2} a_1^2 \int_0^1 \frac{P^2 a_2^2}{P^2} a_2^2 \right] \\ &\quad + \frac{P^2 a^2 b^2}{2P^4 P^4} \left[ \int_0^1 a_1^2 \int_0^1 \frac{P^4 a_2^2}{P^4} a_2^2 \right] \\ &\quad + \frac{P^2 a^2 b^2}{2P^2} \int_0^1 \frac{P^2 a_1^2}{P^2} a_1^2 \int_0^1 P^2 a_2^2 \dots\dots\dots 24 \end{aligned}$$

**3. Direct Variation of Total Potential Energy-** For direct variation, equation (24) shall be differentiated with respect to the deflection coefficient, A and the outcome is:

$$\begin{aligned} \frac{\delta U}{\delta A} &= \frac{P^2}{P^4} \left[ \int_0^1 \frac{P^4 a_1^2}{P^4} a_1^2 \int_0^1 P^2 a_2^2 \right] \\ &\quad + 2 \frac{P^2}{P^4 P^2} \left[ \int_0^1 \frac{P^2 a_1^2}{P^2} a_1^2 \int_0^1 \frac{P^2 a_2^2}{P^2} a_2^2 \right] \\ &\quad + \frac{P^2}{P^4 P^4} \left[ \int_0^1 a_1^2 \int_0^1 \frac{P^4 a_2^2}{P^4} a_2^2 \right] \\ &\quad + \frac{P^2 a^2 b^2}{P^2} \int_0^1 \frac{P^2 a_1^2}{P^2} a_1^2 \int_0^1 P^2 a_2^2 = 0 \end{aligned}$$

That is

$$\begin{aligned} &\frac{P^2}{P^4} \left[ \int_0^1 \frac{P^4 a_1^2}{P^4} a_1^2 \int_0^1 P^2 a_2^2 \right] + 2 \frac{P^2}{P^4 P^2} \\ &\quad + \frac{P^2}{P^4 P^4} \left[ \int_0^1 a_1^2 \int_0^1 \frac{P^4 a_2^2}{P^4} a_2^2 \right] \\ &\quad + \frac{P^2 a^2 b^2}{P^2} \int_0^1 \frac{P^2 a_1^2}{P^2} a_1^2 \int_0^1 P^2 a_2^2 \dots\dots\dots 25 \end{aligned}$$

Equation (25) is the direct governing equation of rectangular plate under buckling using work-error. Rearranging equation (25) and making the critical buckling load,  $N_x$  the subject of the equation gives:

$$w_{\xi} = \left( \frac{w_1^2 w_{\xi} + 2w_1 w_{\xi\xi} + \frac{w_{\xi\xi}^2}{w_1^2}}{w_{\xi\xi\xi}} \right) * \frac{w_{\xi}}{w_1^2} \dots\dots \tag{26}$$

Where

$$w_{\xi} = \int_0^1 \frac{w_1^4 w_{\xi}}{w_1^4} w_{\xi\xi\xi} \int_0^1 w_2^2 w_{\xi\xi} \dots\dots \tag{27}$$

$$w_{\xi\xi} = \int_0^1 \frac{w_1^2 w_{\xi}}{w_1^2} w_{\xi\xi\xi} \int_0^1 \frac{w_2^2 w_{\xi}}{w_1^2} w_{\xi\xi\xi} \dots\dots \tag{28}$$

$$w_{\xi} = \int_0^1 w_1^2 w_{\xi\xi} \int_0^1 \frac{w_2^4 w_{\xi}}{w_1^4} w_{\xi\xi\xi} \dots\dots \tag{29}$$

and

$$w_{\xi\xi} = \int_{\xi} \frac{w_1^2 w_{\xi}}{w_1^2} w_{\xi\xi\xi} \int_{\xi} w_2^2 w_{\xi\xi} \dots \tag{30}$$

**APPLICATION**

Analysis of a classical rectangular thin isotropic plate with:

- 1) Edges 1 & 3 clamped; edges 2 & 4 simply supported using polynomial functions respectively for  $w_x$  and  $w_y$ .
- 2) Edge 1 clamped, edges 2, 3 and 4 simply supported using only polynomial function for both  $w_x$  and  $w_y$

**1. Edges 1 & 3 clamped; edges 2 & 4 simply supported rectangular plate**

The deflection equation,  $w$  and shape function (Ibearugbulem, et.al, 2014) for CSCS rectangular plates are

$$w = w_1 (w_1 - 2w_1^3 + w_1^4)(w_2^2 - 2w_2^3 + w_2^4) \dots \tag{31}$$

Using split-deflection approach, we have

$$w_{\xi} = \sqrt{w_1} (w_1 - 2w_1^3 + w_1^4) \dots\dots\dots \tag{32}$$

$$\eta_{\eta} = \sqrt{\eta} (\eta^2 - 2\eta^3 + \eta^4) \dots\dots\dots 33$$

From equations (32) and (33), shape (profile) functions  $h_1$  and  $h_2$  are:

$$\eta_1 = \eta - 2\eta^3 + \eta^4 \dots\dots\dots 34$$

$$\eta_2 = \eta^2 - 2\eta^3 + \eta^4) \dots\dots\dots 35$$

When we integrate these profile functions, we obtain:

$$\int_0^1 \eta_1^2 \eta \eta = \int_0^1 (\eta^2 - 4\eta^4 + 2\eta^5 + 4\eta^6 - 4\eta^7 + \eta^8) \eta \eta$$

$$\frac{\eta^3}{3} - \frac{4\eta^5}{5} + \frac{2\eta^6}{6} + \frac{4\eta^7}{7} - \frac{4\eta^8}{8} + \frac{\eta^9}{9}$$

$$\frac{1}{3} - \frac{4}{5} + \frac{2}{6} + \frac{4}{7} - \frac{4}{8} + \frac{1}{9} = \frac{31}{630}$$

$$\eta \eta \eta \int_0^1 \eta_2^2 \eta \eta = \int_0^1 (\eta^4 - 4\eta^5 + 6\eta^6 - 4\eta^7 + \eta^8) \eta \eta$$

$$\frac{\eta^5}{5} - \frac{4\eta^6}{6} + \frac{6\eta^7}{7} - \frac{4\eta^8}{8} + \frac{\eta^9}{9} \Big|_0^1$$

$$\frac{1}{5} - \frac{4}{6} + \frac{6}{7} - \frac{4}{8} + \frac{1}{9} = \frac{1}{630}$$

Similar procedure was adopted to obtain the values

$$\int_0^1 \frac{\eta^4 \eta_1}{\eta \eta^4} \eta_1 \eta \eta = \frac{24}{5} \eta \eta \eta \int_0^1 \frac{\eta^4 \eta_2}{\eta \eta^4} \eta_2 \eta \eta = \frac{4}{5}$$

$$\int_0^1 \frac{\eta^2 \eta_1}{\eta \eta^2} \eta_1 \eta \eta = \frac{17}{35} \eta \eta \eta \int_0^1 \frac{\eta^2 \eta_2}{\eta \eta^2} \eta_2 \eta \eta = \frac{2}{105}$$

$$\eta_{\eta} = \left(\frac{24}{5}\right) \left(\frac{1}{630}\right) = \frac{4}{525} \dots\dots\dots 36$$

$$\eta_{\eta \eta} = \left(\frac{17}{35}\right) \left(\frac{2}{105}\right) = \frac{34}{3675} \dots\dots\dots 37$$

$$\begin{aligned} \delta_{\delta} &= \left(\frac{31}{630}\right)\left(\frac{4}{5}\right) \\ &= \frac{123}{3125} \dots\dots \end{aligned} \tag{38}$$

and

$$\begin{aligned} \delta_{\delta\delta} &= \left(\frac{17}{35}\right)\left(\frac{1}{630}\right) \\ &= \frac{17}{22050} \dots \end{aligned} \tag{39}$$

Substituting equations (38) to (39) into equation (26) gives

$$\begin{aligned} \delta_{\delta} &= \left(\frac{0.007617\delta^2 + 2 * \left(\frac{34}{3675}\right) + \frac{0.03936}{\delta^2}}{0.0007708}\right) * \frac{\delta}{\delta^2} \\ \delta_{\delta\delta} &= \left(9.88194\delta^2 + 24.00545 + \frac{51.06383}{\delta^2}\right) * \frac{\delta}{\delta^2} \dots\dots\dots \end{aligned} \tag{40}$$

**2. Edge 1 clamped & edges 2, 3 & 4 simply supported rectangular plate**

The deflection equation, w and the shape function H for CSSS rectangular plates are

$$\delta = \delta (\delta - 2\delta^3 + \delta^4)(1.5\delta^2 - 2.5\delta^3 + \delta^4)\dots \tag{41}$$

Using split-deflection approach, we have

$$\delta_{\delta} = \sqrt{\delta} (\delta - 2\delta^3 + \delta^4) \dots\dots\dots \tag{42}$$

$$\delta_{\delta} = \sqrt{\delta} (1.5\delta^2 - 2.5\delta^3 + \delta^4) \dots\dots\dots \tag{43}$$

From equations (42) and (43), h<sub>1</sub> and h<sub>2</sub> are:

$$\begin{aligned} \delta_1 &= \delta - 2\delta^3 \\ &+ \delta^4 \dots\dots\dots \end{aligned} \tag{44}$$

$$\delta_2 = 1.5\delta^2 - 2.5\delta^3 + \delta^4 \dots\dots\dots \tag{45}$$

With these equations, we obtain:

$$\begin{aligned}
 \int_0^1 x_1^2 dx &= \int_0^1 (x - 2x^3 + x^4)^2 dx \\
 &= \int_0^1 (x^2 - 4x^4 + 2x^5 + 4x^6 - 4x^7 + x^8) dx \\
 &= \frac{x^3}{3} - \frac{4x^5}{5} + \frac{2x^6}{6} + \frac{4x^7}{7} - \frac{4x^8}{8} + \frac{x^9}{9} \\
 \frac{1}{3} - \frac{4}{5} + \frac{2}{6} + \frac{4}{7} - \frac{4}{8} + \frac{1}{9} &= \left(\frac{31}{630}\right)
 \end{aligned}$$

$$\begin{aligned}
 \int_0^1 x_2^2 dx &= \int_0^1 (1.5x^2 - 2.5x^3 + x^4)^2 dx \\
 &= \int_0^1 (2.25x^4 - 7.5x^5 + 9.25x^6 - 5x^7 + x^8) dx
 \end{aligned}$$

$$\begin{aligned}
 &\left(\frac{2.25x^5}{5} - \frac{7.5x^6}{6} + \frac{9.25x^7}{7} - \frac{5x^8}{8} + \frac{x^9}{9}\right) \Big|_0^1 \\
 \frac{2.25}{5} - \frac{7.5}{6} + \frac{9.25}{7} - \frac{5}{8} + \frac{1}{9} &= 19/2520
 \end{aligned}$$

$$\int_0^1 \frac{x_1^4}{x^4} dx = 4.8 \int_0^1 \frac{x_2^4}{x^4} dx = \frac{9}{5}$$

$$\int_0^1 \frac{x_1^2}{x^2} dx = \frac{17}{35} \int_0^1 \frac{x_2^2}{x^2} dx = \frac{3}{35}$$

$$\begin{aligned}
 x_{11} &= (4.8) \left(\frac{19}{2520}\right) \\
 &= \frac{19}{525} \dots\dots \quad 46
 \end{aligned}$$

$$x_{21} = \left(\frac{17}{35}\right) \left(\frac{3}{35}\right) = \frac{51}{1225} \dots\dots \quad 47$$

$$x_{12} = \left(\frac{31}{630}\right) (1.8) = \frac{279}{1350} \dots\dots \quad 48$$

$$x_{22} = \left(\frac{17}{35}\right) \left(\frac{19}{2500}\right) = \frac{323}{88200} \dots\dots \quad 49$$

Substituting equations (46) to (49) into equation (26) gives

$$P_{cr} = \left( \frac{0.03619P^2 + 2 * 0.041633 + \frac{0.088571}{P^2}}{0.0036621} \right) * \frac{P}{P^2}$$

.....

$$P_{cr} = \left( 9.88231P^2 + 22.73723 + \frac{24.1859}{P^2} \right) * \frac{P}{P^2} \dots\dots\dots 50$$

**RESULTS**

The non-dimensional form of the critical buckling loads for different aspect ratios for cscs and csss plates are shown on tables 1 and 2. Figures 1 and 2 present same result in graphical form.

**Table 1: Non-dimensional form of critical buckling load of CSCS isotropic thin plate**

| Aspect ratio, P | Critical buckling load, Nx $\left(\frac{P}{P^2}\right)$ |                                  | Percentage difference |
|-----------------|---|----------------------------------|-----------------------|
|                 | Present   | Past (Ibearugbulem et al., 2014) |                       |
| 1               | 84.95   | 85.06494                         | 0.135                 |
| 1.1             | 78.16   | 78.27207                         | 0.143                 |
| 1.2             | 73.70   | 73.80192                         | 0.138                 |
| 1.3             | 70.92   | 71.0267                          | 0.150                 |
| 1.4             | 69.426  | 69.53446                         | 0.1560                |
| 1.5             | 68.933  | 69.04582                         | 0.163                 |
| 1.6             | 69.248  | 69.36585                         | 0.170                 |
| 1.7             | 70.231  | 70.35524                         | 0.176                 |
| 1.8             | 71.780  | 71.91225                         | 0.184                 |
| 1.9             | 73.821  | 73.96119                         | 0.1895                |
| 2.0             | 76.295  | 76.44481                         | 0.1960                |

$$P_{cr} = \left( 9.88P^2 + 24.01 + \frac{51.06}{P^2} \right) * \frac{P}{P^2}$$

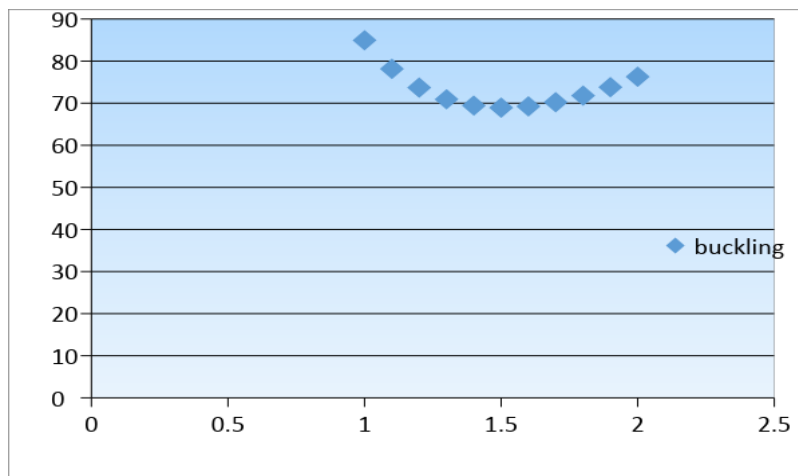


Figure 1.0: The Graph of Non-Dimensional Buckling Load against Aspect Ratio (CSCS plate).

**Table 2: Non-dimensional form of critical buckling load of CSSS isotropic thin plate**

| Aspect ratio, P | Critical buckling load, $N_x \left( \frac{a}{b} \right)$ |                                     | Percentage difference |
|-----------------|--|-------------------------------------|-----------------------|
|                 | Present  | Past<br>(Ibearugbulem et al., 2014) |                       |
| 1               | 56.810   | 56.80234                            | 0.014                 |
| 1.1             | 54.687   | 54.68031                            | 0.013                 |
| 1.2             | 53.766   | 53.76084                            | 0.018                 |
| 1.3             | 53.751   | 53.74698                            | 0.007                 |
| 1.4             | 54.447   | 54.44388                            | 0.006                 |
| 1.5             | 55.721   | 55.71938                            | 0.004                 |
| 1.6             | 57.482   | 57.4813                             | 0.002                 |
| 1.7             | 59.663   | 59.66373                            | 0.002                 |
| 1.8             | 62.217   | 62.21855                            | 0.003                 |
| 1.9             | 65.108   | 65.10996                            | 0.003                 |
| 2.0             | 68.308   | 68.31088                            | 0.004                 |

$$\frac{N_x}{a} = \left( 9.88a^2 + 22.74 + \frac{24.19}{a^2} \right) \cdot \frac{a}{a^2}$$

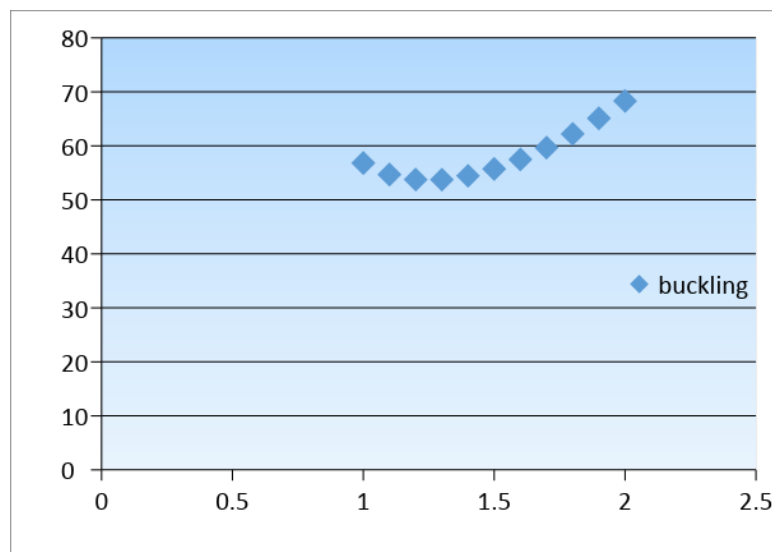


Figure 2.0: The Graph of non-dimensional Buckling Load against Aspect Ratio (CSSS plate)

In the case of CSCS thin plates, that is table 1, for the aspect ratio of 1.0, the buckling load was 84.95. For the aspect ratio of 2.0, the buckling load was 76.295. From the table; it can be observed that as the aspect ratio increased from 1.0 to 2.0, the buckling load decreased from 84.95 to 76.295. Therefore, for an increment of 1.0 (1.0-2.0) aspect ratio, there was a decrease of 8.66 non-dimensional form of buckling load.

Table 2 shows results for CSSS Isotropic Thin Plates. For the aspect ratio of 1.0, the buckling load was 56.81. It decreased to a point corresponding to the aspect ratio of 1.5. It gradually increased again at aspect ratio of 2.0. Therefore, for an aspect ratio of 1.0 to 1.5, there was a decrease of 1.089 non-dimensional form of buckling load. For the aspect ratio of 1.6 to 2.0, there was an

increase of 10.826 non-dimensional form of buckling load. This variation in buckling load can be attributed to the plate boundary configuration and restraint conditions.

From the graph of Figure 1.0, the buckling load,  $P_{cr}$  graph becomes parabolic at an aspect ratio of 1.5. Obviously, this could be attributed to the boundary condition (restraint) of the plate. Which means for different plate geometry/configuration, the buckling load, ( $P_{cr}$ ) vis-a-viz, the aspect ratio changes.

In Figure 2.0, at the origin of the curve, the aspect ratio was 1.0 with non-dimensional buckling load of 56.810. The graph descended gradually to non-dimensional buckling load of 55.721. This corresponded to an aspect ratio of 1.5. The descent of the curve was very steep. The ascent corresponds to the aspect ratio of 1.6 and continues to 2.0 with non-dimensional buckling load of 68.308. This variation in buckling load can be attributed to the plate boundary configuration and restraint conditions.

### CONCLUSIONS AND RECOMMENDATIONS

A critical examination of the tables reveals that the maximum percentage difference between the values from the present study and those from Ibearugbulem et, al. (2014) is 0.196. This value of the difference may be due to round off error. Statistically, the implication is, that no difference exists between the two sets of values. Thus, one can infer that the procedure, the profile functions and the energy functions formulated in this present study are reliable and sufficient in CPT buckling analysis of rectangular plates. From the findings of this study, this method is recommended for stability analysis of CPT plates.

A further study for use of the present method in refined plate theory analysis (RPT) is also recommended.

This study therefore developed an alternative equation option to the single orthogonal deflection equations already in use in plates analysis. It successfully applied the split-deflection method in the analysis of thin isotropic rectangular plates- that is a new plate buckling concept where a rectangular plate is split into two independent and distinct components x and y, where the deflection of the rectangular plate becomes the product of these two components x and y ( $w = w_x * w_y$ ).

**REFERENCES**

- Erdem, C. Imrak and Ismail Gerdemeli (2007).** The problem of isotropic rectangular plate with four clamped edges. *S-adhan-a* Vol. 32, Part 3, pp. 181–186.
- Ezeh, J. C., Ibearugbulem, O. M., Njoku, K. O., and Ettu, L. O. (2013).** Dynamic Analysis of Isotropic SSSS Plate Using Taylor Series Shape Function in Galerkin's Functional. *International Journal of Emerging Technology and Advanced Engineering*, 3 (5): 372-375.
- Hutchinson, J. R. (1992).** On the bending of rectangular plates with two opposite edges simply supported. *J. Appl. Mech. Trans. ASME* 59: 679–681.
- Ibearugbulem, Owus, M; Ibearugbulem, C.N., Momoh Habib and Asomugha A.U. (2016).** Buckling Analysis of Rectangular Plates by Split-Deflection Method. *International Journal of Emerging Technology and Advanced Engineering*, Vol 3 (5): Pp 27-30.
- Ibearugbulem, O. M. (2014).** Using the product of two mutually perpendicular truncated polynomial series as shape function for rectangular plate analysis, *International Journal of Emerging Technologies and Engineering (IJETE)* ISSN: 2348–8050, ICRTIET-2014 Conference Proceeding, 30th -31st August 2014, 1-4
- Jiu, Hui Wu, A. Q. Liu, and H. L. Chen (2007).** Exact Solutions for Free-Vibration Analysis of Rectangular Plates. *Journal of Applied Mechanics* Vol. 74 pp. 1247-1251.
- Njoku, K. O., Ezeh, J. C., Ibearugbulem, O. M., Ettu, L. O., and Anyaogu, L. (2013).** Free Vibration of Thin Rectangular Isotropic CCCC Plate Using Taylor Series Formulated Shape Function in Galerkin's Method. *Academic Research International*, 4 (4): 126-132.
- Szilard, R. (2004).** *Theories and Applications of Plate Analysis*. New Jersey: John Wiley & Sons Inc.
- Taylor, R. L. and S. Govindjee (2004).** Solution of clamped rectangular plate problems. *Communi. Numer. Meth. Eng.* 20: 757–765.
- Ugural, A. C. (1999).** *Stresses in plates and shells*, 2nd ed. Singapore: McGraw-hill.
- Ventsel, E. and T. Krauthammer (2001).** *Thin Plates and Shells: Theory, Analysis and Applications*. New York: Marcel Dekker.
- Wang, C. M., Y. C. Wang, and J. N. Reddy (2002).** Problems and remedy for the Ritz method in determining stress resultant of corner supported rectangular plates. *Comput. Struct.* 80: 145–154
- Ye, Jianqiao (1994).** Large deflection of imperfect plates by iterative BE-FE method. *Journal of Engineering Mechanics*, Vol. 120, No. 3 (March).